The Relationship Between Multiple Hazards and Deprivation Using Open Geospatial Data and Machine Learning

Priscilla Kabiru
ITC: Universiteit Twente Faculteit Geo-Informatie Wetenschappen en Aardobservatie
Monika Kuffer (m.kuffer@utwente.nl)
University of Twente Faculty of Geo-Information Science and Earth Observation: Universiteit Twente Faculteit Geo-Informatie Wetenschappen en Aardobservatie https://orcid.org/0000-0002-1915-2069
Richard Sliuzas
ITC: Universiteit Twente Faculteit Geo-Informatie Wetenschappen en Aardobservatie
Sabine Vanhuysse
Free University of Brussels: Universite Libre de Bruxelles

Research Article

Keywords: Slum, informal settlement, hazards, vulenerabiliy, deprivation

Posted Date: February 22nd, 2022

DOI: https://doi.org/10.21203/rs.3.rs-1359834/v1

Title Page

THE RELATIONSHIP BETWEEN MULTIPLE HAZARDS AND DEPRIVATION USING OPEN GEOSPATIAL DATA AND MACHINE LEARNING

Priscilla Kabiru[1], Monika Kuffer[1], Richard Sliuzas[1] and Sabine Vanhuysse[2]

[1] Faculty of Geo-Information Science and Earth Observation (ITC), University of Twente, 7514 AE Enschede, The Netherlands; priscillakabiru@gmail.com (PK); m.kuffer@utwente.nl (MK); r.sliuzas@utwente.nl (RS)

[2] Department of Geosciences, Environment and Society, Université Libre de Bruxelles (ULB), 1050 Brussels, Belgium; sabine.vanhuysse@ulb.be (SB)

Abstract

Deprived settlements, usually referred to as slums, are often located in hazardous areas. However, there have been very few studies to examine this notion. In this study, we leverage the advancements in open Geospatial data, Earth Observation (EO), and machine learning to create a multi-hazard index and transferrable disaster risk approach to be adapted in LMICs cities, with low-cost methods. Specifically, we identify multi-hazards in Nairobi's select case study area and construct an index. Then, we test the predictability of deprived settlements using the multi-hazard index in comparison to EO texture-based methods. Lastly, we survey 100 households in two deprived settlements (typical and atypical slum) in Nairobi and used the survey outcomes to validate the multi-hazard index. To test the assumption that deprived areas are dominantly located in areas with higher susceptibility to multiple hazards, we contrast morphologically identified deprived settlements to non-deprived settlements. We find that deprived settlements are generally more exposed to hazards. However, there are variations between central and peripheral settlements. In testing the predictability of deprivation using multi-hazards, the model performs well at classifying deprivation compared to other morphological settlement classes. Specifically, we find the model to perform better at discriminating deprivation in comparison to other morphological settlements. In contrast, the texture-based model is better at classifying all morphological settlements. Lastly, by contrasting the survey outcomes to the household interviews, we conclude that proxies used for the multi-hazard index adequately capture the hazards. However, more localized proxies can be used to improve multi-hazard index performance.

Keywords

Slum; informal settlement; hazards; vulenerabiliy; deprivation;

Acknowledgements

We would like to express our gratitude to Diana Reicken, Nicholus Mboga, Angela Abascal, Stefanos Georganos and Maxwell Owusu for providing feedbacks during the conceptual phase of this reseach. Furthermore, we would like to acknowledge the valuable input of the IDEAMAPs team, provided data for the research; the team at the Department of Geography; King's College London, Strand Campus: Prof. Mark Pelling, Bruce D. Malamud, Robert Sakic Trogrlic and Sebastiaan Beschoor Plug who provided helpful input on hazard analysis, including providing relevant literature and; the local organizations – Community Mappers and Spatial Collective for the help in collecting data. Maria Isabel Arango, a hazard specialist for refining the hazard analysis, Brian Masinde and Alfredo Chavarria reviewed the algorithms used in this study and Gift Kyansimire to illustrate Nairobi.

Funding

The principal author received research support from the Faculty Geo-Information Science and Earth Observation, University of Twente ITC Foundation. Additionally, research pertaining to these results received financial aid from the Belgian Federal Science Policy (BELSPO) according to the agreement of subsidy no. SR/11/380 (SLUMAP). (SLUMAP: http://slumap.ulb.be/) and from NWO grant number VI. Veni. 194.025.

Author Contributions

All authors contributed to the study conception and design. Material preparation, data collection and analysis were performed by Priscilla Kabiru and reference data were prepared by Sabine Vanhuysse. The first draft of the manuscript was written by Priscilla Kabiru and Monika Kuffer and all authors commented on previous versions of the manuscript. All authors read and approved the final manuscript.

THE RELATIONSHIP BETWEEN MULTIPLE HAZARDS AND DEPRIVATION USING OPEN GEOSPATIAL DATA AND MACHINE LEARNING

1. Introduction

Globally, disasters lead to massive economic losses, displacements, injuries and fatalities (Dilley et al., 2005; EM-DAT, 2009). These concentrate in cities and particular cities located in Low-and-Middle-Income Countries (LMICs). Commonly, studies focus on a specific hazard and analyze disaster risks; however, most cities are affected by multiple hazards (Dilley et al., 2005). Data to support multiple hazard analyses in LMIC cities are often not readily available, limiting the spatial knowledge on intracity patterns of multiple hazard susceptibility and its relation with urban inequality (deprivation).

Disasters are commonly caused by man-made, natural and technological hazards causing damage and losses (Gallina et al., 2016). Notably, urban areas are hotspots for anthropogenic activities that have resulted in increased hazards. For instance: increased impervious surfaces (Seto, Sánchez-Rodríguez, & Fragkias, 2010), destruction of natural ecosystems (Seto & Shepherd, 2009) and; increased heat-trapping greenhouse gases (GHG) that have significantly contributed to global warming (Revi, Satterthwaite, et al., 2014). Also, many cities globally are located in hazard-prone regions. Additionally, more than 50% of the world's population reside in urban areas (United Nations, 2019); therefore, hazards represent a significant issue of risk for humanity.

Further, inequality (i.e., the economic polarisation between the wealthy and the poor) characterizes many LMIC cities (Phillips et al., 2007), and urban poverty has been spatially manifested as slums settlements (non-exclusively) (Baker, 2008; UN-Habitat, 2015). One in eight urban dwellers live in a slum (UN-Habitat, 2015), and in Sub-Saharan Africa (SSA), 59% of the urban population are slum residents (UN-Habitat, 2015). Typically, slums settlements are characterised by their poor environmental living conditions. Physically, slums are characterized by structures built without (if any) regard for building codes and are of poor material with low structural integrity. Failing to provide the inhabitants with adequate protection from harsh climatic conditions. Spatially, slum settlements are contiguous, overcrowded with irregular patterns, and lacking adequate infrastructure. They are located on derelict land and low environmental quality areas like near highways and industrial areas (Ramin, 2009; Wekesa, Steyn, & Otieno, 2011). Often they are deprived of green spaces (vegetation) to act as natural sinks for pollutants and excess precipitation and thus have low air quality and are prone to flooding. Geographically, these settlements are situated in hazardous locations. For instance, on flood plains and steep hills prone to floods and landslides, respectively. These characteristics default the urban poor to the forefront of disaster risks (Revi et al., 2014; Phillips et al., 2007).

Presently, cities are affected by more than one hazard, and the frequency of disasters is reportedly increasing (Dilley et al., 2005). However, studies on multiple hazards in cities have been limited due to the focus on single hazards (e.g., J. Wang, Kuffer, Sliuzas, & Kohli, 2019; S. Wang, Wang, Fang, & Feng, 2019). In LMIC's especially, data to support multiple hazard studies is scarce, and often limited to small areas such as neighbourhoods (e.g., Mulligan, Harper, Kipkemboi, Nobi, & Collins, 2017). However, advancements in open Geospatial data, Earth Observation (EO), and machine learning can help to address these limitations. As a framework for analyzing multi-hazards, indices have proven robust in handling heterogeneous spatial data (e.g. Dilley et al., 2005; Greiving, 2006). Also, several studies showed the potential to combine EO data and geospatial data using innovations in machine learning (e.g., Kuffer, Pfeffer, & Sliuzas, 2016; Ajami, Kuffer, Persello, & Pfeffer, 2019; Müller et al. 2020). Therefore, this study analyses the relationship between hazards and deprivation using a multi-hazard approach using the city of Nairobi as a case study to analyze this relationship, because of data availability. Furthermore, like other studies (see Kuffer et al., 2020, 2018; Thomson et al., 2020), we adopt the term deprived areas (and its variants) to refer to slums.

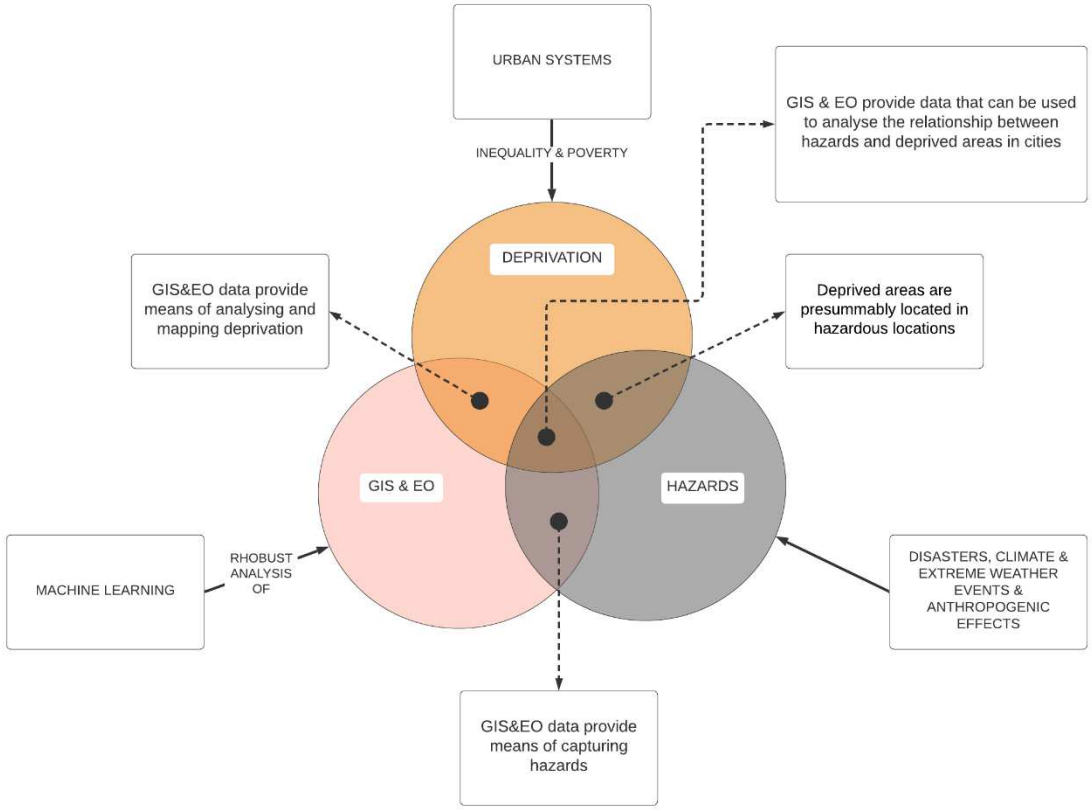

Figure 1: Relationship between hazard and deprivation analysed with Geospatial and Earth Observation (EO) data.

2. Methodology

To analyse the relationship between hazards and deprivation, we contextualize the aforementioned environmental conditions of deprived areas using the generic slum ontological (GSO) framework developed by Kohli et al. (2012) (Fig.2). Utilizing the hierarchical grouping nature of the framework, we identify three spatial levels (environs-city, settlement, and object-household level) for our analysis.

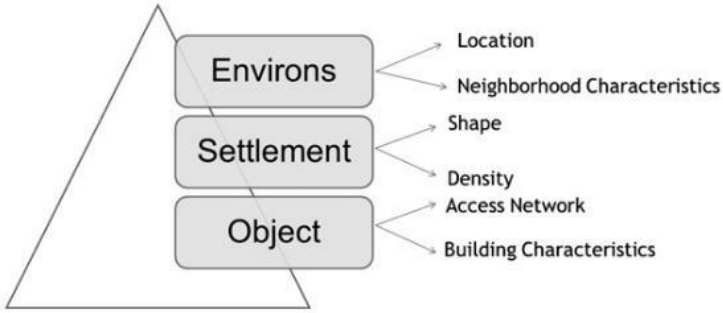

Figure 2: Generic Slum Ontological (GSO) framework (Kohli et al. 2012).

At the city level, we use open geospatial and processed EO data (available in open archives) to construct a multiple hazard index (Fig.3). The use of open data will support the transferability and scalability of the proposed index beyond the case study area. Thus a multi-hazard index is constructed, using relevant local indicators and open Geospatial and EO data; this selection is informed by extensive literature review and key informant interviews. By consulting the experts, we gain insights into the hazards present in the study area and thus refine the theoretical

multi-hazard index. We conduct extensive literature and database search to identify geo-data to construct the index.

Next, we test the assumption that deprived settlements are located in hazardous areas in cities – an assumption that presumes a direct relationship between hazards and deprivation. To do this, we first compute descriptive statistics on the multi-hazard index to analyze the relationship between hazards and the different settlements in our study area. Secondly, we use machine learning methods to analyze whether the multi-hazard index can predict deprivation. We use the multi-hazard index developed in the first step to perform a land-use classification of the different types of residential settlements (and other identified land uses) in our study area. In parallel, we also run an experiment using a common land use classification method, i.e., using textural features as a control test. Lastly, we conduct household interviews to analyze the inter-settlement hazard dispersal and household-level exposure to hazards. The household survey findings are contrasted with the outcome of the multi-hazard index.

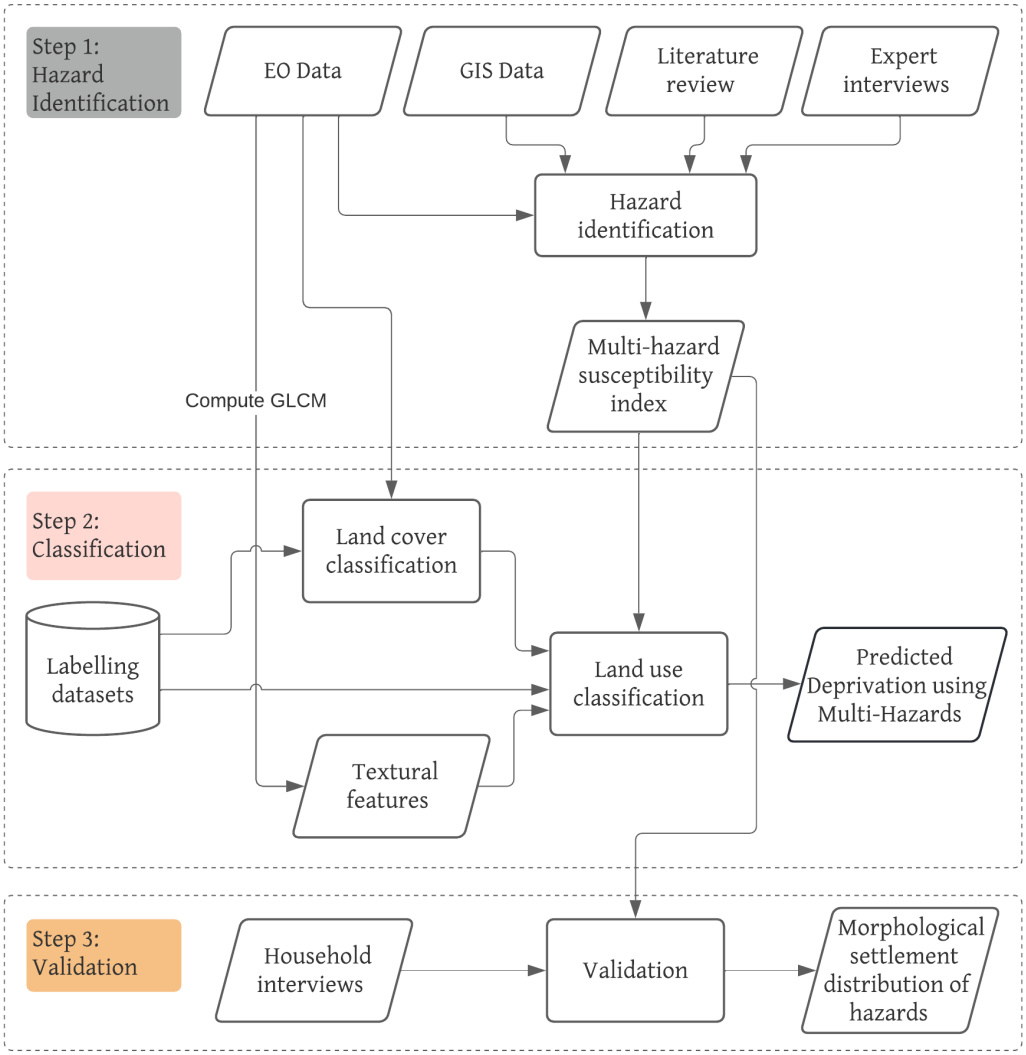

Figure 3:Overview of the methodology.

a. Case study – Nairobi, Kenya

Nairobi (Fig. 4), the capital city of Kenya, has a population of 4.4 million people (Kenya National Bureau of Statistics, 2019). The city has a high level of inequality in terms of housing, infrastructure, services, etc., dating back to the pre-independence racial zoning and rigid building standards (Gatabaki-Kamau & Karirah-Gitau, 2004; Pamoja Trust, 2009). After independence in 1963, Nairobi experienced a housing crisis leading to the massive growth of high-density deprived areas. The housing privatization legislation worsened the situation. Presently, approximately 86% of Nairobi's housing stock is supplied by the private sector, including slumlords (KNBS,

2018). It is estimated that around 60% of the inhabitants of Nairobi live in deprived settlements that occupy 4% of the built-up area (Pamoja Trust, 2009).

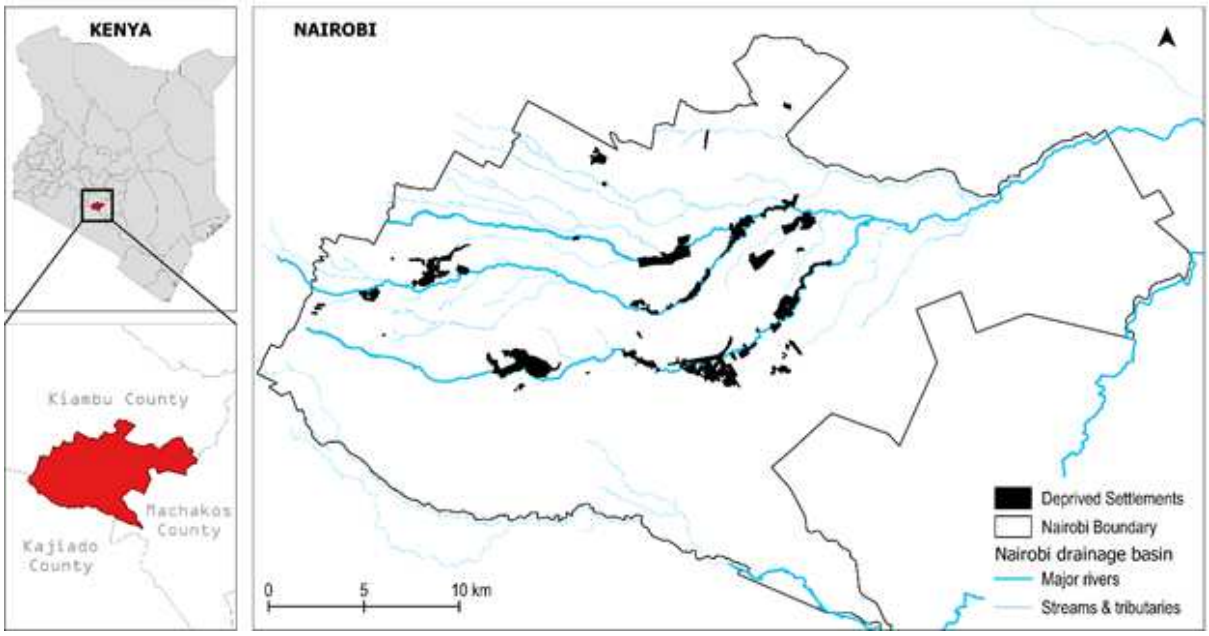

Figure 4: Case study area – Nairobi (Sources: GADM & Spatial collective).

However, deprived urban areas in Nairobi are not homogenous; we used in total four different types of residential areas (Fig. 5):

- Class 1: High to mid-density built area, formal central housing areas
- Class 2: Low density built area, commonly single-family housing mainly at the periphery
- Class 3: Deprived urban area (Type I), typical slums, very densely built-up areas commonly at more central locations
- Class 4: Deprived urban area (Type II), atypical slums, high to mid-density built-up areas commonly at the periphery

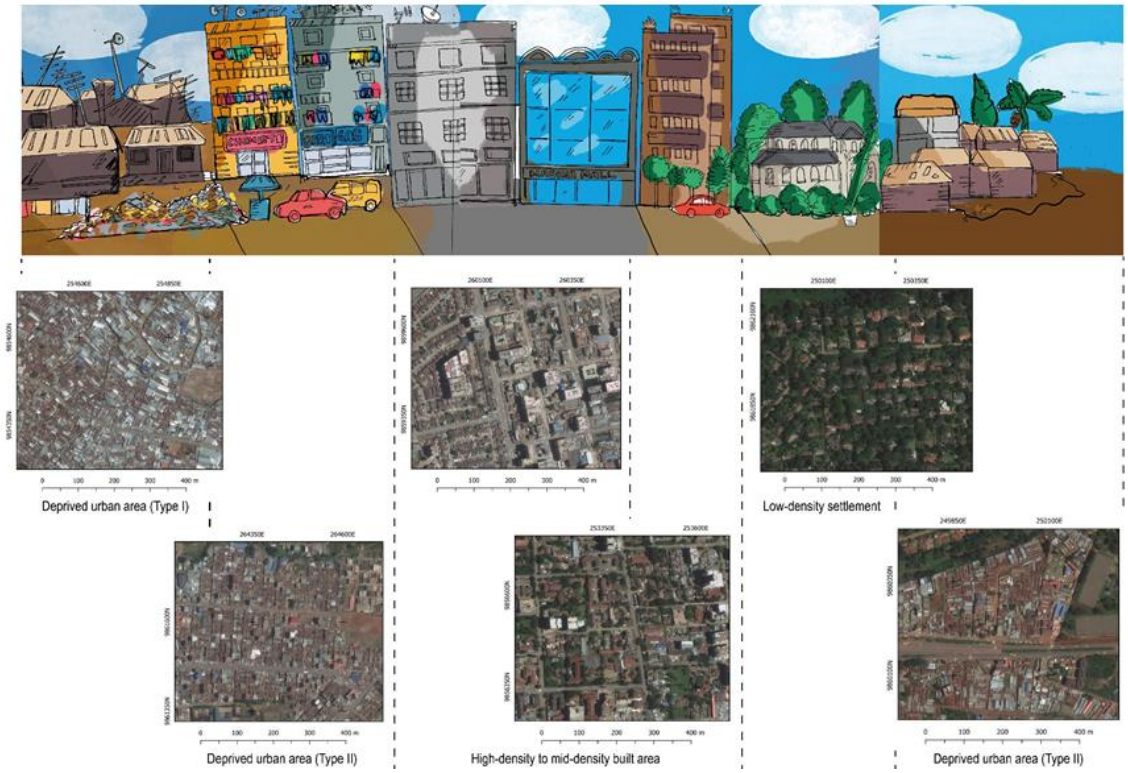

Figure 5: Four types of residential areas in Nairobi as used in this study.

b. Data and software

To define our area of interest (AOI), we select Nairobi county's (which is also the city's) political-administrative boundary (fig.4) obtained from GADM. Additionally, we obtain cloud-free Sentinel 2 surface reflectance multispectral imagery from European Space Agency (ESA). The imagery is downloaded using Google Earth Engine (GEE) for 2019, where the annual mean values are computed, and cloud masking is also undertaken. A similar approach is undertaken to acquire Land Surface Temperature from MODIS and air pollution data from Sentinel 5P, where the annual maximum values are computed. The Digital Elevation Model (DEM), a Synthetic Aperture Radar (SAR) Radiometric Terrain Corrected (RTC), imagery is obtained from the National Aeronautics and Space Administration (NASA) Earth Data portal. Nairobi's land use map and building outlines were generated by Columbia University's Center for Sustainable Urban Development in 2010 and obtained through the World Bank data portal. The slum boundaries were obtained from a local company – Spatial Collective, and represent morphological slums. Ancillary data was obtained from Open Street Map (OSM). ESRI satellite imagery, accessed through QGIS, is used as a base map and conceptualizes settlements. Free and Open Source Software for Geoinformatics (FOSS4G) solutions are employed in our study. Specifically, QGIS is used for raster and vector data manipulation, KoBo Toolbox for primary data collection (household questionnaires), and R studio for advanced statistical manipulation, i.e., texture extraction and machine learning (annex.8.5). We, however, also use commercial software: ArcGIS 10.8.1-Topography Toolbox (Tom Dilts, 2015) for extracting the Height Above Nearest Drainage (HAND); ZOOM – a video teleconferencing platform for conducting key informant interviews; MS-Excel and SPSS for statistical analysis of our data. MS Excel is also used to present the outcomes of the statistical analysis.

c. Construction of a Multi-Hazard Susceptibility Index

To develop and localize a multi-hazard index, we used the Emergency Events Database (EM-DAT) (EM-DAT, 2009) classification of disasters. We related it to UN-Habitats' measures of durable housing, where we identify two broad hazard domains, i.e., natural and technological hazards (Table 1). Furthermore, we review the country's

National Policy for Disaster Management (Government of Kenya, 2009), the "Tomorrow's Cities: Urban risk in transition" project under current implementation in Nairobi, the IDEAMAPs framework of Domains of Deprivation (Abascal et al., 2021) and conduct expert interviews to identify hazards affecting our study area at the city and deprived settlement.

Table 1: Hazard domain derivation from UN-Habitat 'Durable Housing' measures.

Hazard group	**Hazard sub-group**	**Description** (EM-DAT, 2009)	**UN-Habitat durable housing measures**
Natural	Hydrological, e.g., floods and landslides	'A hazard caused by the occurrence, movement, and distribution of surface and subsurface freshwater and saltwater.'	Housing in geologically hazardous zones (landslide/ earthquake and flood areas)
	Geophysical, e.g., earthquake and volcanic activity	'A hazard originating from solid earth. This term is used interchangeably with the term geological hazard.'	
	Biological, e.g., epidemic	'A hazard caused by the exposure to living organisms and their toxic substances (e.g. venom, mould) or vector-borne diseases that they may carry.'	Housing on or under garbage mountains
	Meteorological, e.g., extreme temperature	'A hazard caused by short-lived, micro- to mesoscale extreme weather and atmospheric conditions that last from minutes to days.'	Quality of construction (e.g. materials used for wall, floor and roof)
Technological	Transport, e.g., air, rail and road	'A hazard caused by transport-related accidents or incidents.'	Housing around other unprotected high-risk zones (e.g. railroads, airports, energy transmission lines)
	Industrial, e.g., pollution and explosions	'A hazard caused by industry-related accidents or incidents.'	Housing around high-industrial pollution areas
	Miscellaneous, e.g., fire and building collapse	'Any other hazard which may cause harm to a population or destruction of assets/property.'	Compliance with local building codes, standards and bylaws.

We develop a multi-hazard index using the spatial multi-risk index construction principles outlined by Greiving (2006), which are: (i) non-sectoral, meaning the consideration of hazards should incorporate different sectors; (ii) the hazards should have spatial relevancy; and (iii) collective hazards are what should be considered. To construct the index, we identify open geospatial data indicative of hazardousness following extensive literature search and outcomes of the expert interviews. The identified geospatial and EO-based variables result in 6 major hazard groups disaggregated into 10 sub-hazards(indicator groups) and 18 sub-hazard indicators (Table 2).

We assign equal weights to each of our six main hazard groups. Thus, each hazard group is accorded equal importance. Equal weightage is considered since we lack access to data that could be used to compute the weights (e.g., frequency of hazards). The weights are then distributed among the sub-hazard groups and all 18 data indicators (Table 2). Additionally, we resample all the data to 10m, our chosen unit of operation, for consistency purposes- given that we rely on Sentinel 2 data (10m resolution) for further analysis (next section).

Table 2: Hazard indicators, their descriptions and properties.

Hazard	Sub-Hazard	Code	Indicator	Description	Resolution	Measurement	Data Source
Flood	Riverine floods	F1	Height Above Nearest Drainage (H.A.N.D)	Height relationship of locations to nearest natural drainage (extract of DEM)	12.5m	Vertical distance (m)	ALOS PALSAR -NASA
		F2	Proximity to Rivers	Distance from major river drainage system of the city	10m	Euclidean distance (m)	OSM
	Run-off	F3	Geomorphons	Terrain form of the city extracted from DEM	12.5m	Classified absolutes values	ALOS PALSAR - NASA
Epidemic	Epidemic	E4	Proximity to Garbage dump sites	Distance from the city's dumpsite/landfill	10m	Euclidean distance (m)	OSM
Weather and climate	Extreme temperatures	W5	Day Land Surface Temperature (LST)	Daytime radiative temperature of the city	1000m	Kelvin (K)	MODIS - NASA
		W6	Night Land Surface Temperature (LST)	Night-time radiative temperature of the city			
Transport accidents	Rail accidents	T7	Proximity to Railway lines	Railway lines cutting through the city	10m	Euclidean distance (m)	OSM
	Road accidents	T8	Proximity to major roads	Major roads and highways of the city	10m		
	Aero accidents	T9	Proximity to Airports	Airport boundaries/runways and infrastructure	10m		
Industrial accidents	Industrial accidents	J10	Proximity to Industries	Proximity to industries	10m		
		J11	Density of industries	Number of industries outlines per unit area ($1km^2$)	10m	Density (No. of features/km^2)	Land use map - Columbia University
Biophysical hazards	Fire	B12	Density of buildings	Number of building outlines per unit area ($1km^2$)	10m		Columbia University
		B13	Road density	Number of roads (line segments) per unit area ($1km^2$)	10m		OSM
		B14	NDVI	Density of plant growth	0.01 arc degrees (approx. 11.1 km)	mol/m^2	Sentinel 2 - ESA
	Air pollution	B15	Sulphur Dioxide (SO_2)	Vertical pollutant column density - a ratio of pollutant and total air mass factor			Sentinel 5P - ESA
		B16	Nitrogen Dioxide (NO_2)				
		B17	Ozone (O_3)				
		B18	Carbon Monoxide (CO)				

After identifying relevant data for producing the indicators, we pre-process the data, including projecting the data to Nairobi's Coordinate Reference System (EPSG:32737), masking and clipping to our AOI, resampling to 10m (the same resolution as Sentinel 2 data and normalizing all data (resulting in values ranging from 0 to 1 - lowest to highest indication of hazardousness). An equal number of samples (n=86) are selected for each settlement class to compare the spatial distribution of hazards in Nairobi.

d. Predicting Deprivation via the Multi-Hazard Index

We test the assumption that deprived areas are dominantly the locations with higher susceptibility to multiple hazards. For this purpose, we compare a land cover/use classification based on Sentinel-2 data with a second classification that includes the multiple hazard index.

For the first land cover/user classification, besides the image bands (using 10m resolution Sentinel-2 red, green, blue, and near-infrared (NIR) bands eight), we use eight common textural measures (Haralick, Dinstein, & Shanmugam, 1973; Kuffer, Pfeffer, & Sliuzas, 2016). These textural features are: Contrast, Entropy, Mean, Dissimilarity, Homogeneity, Angular Second Moment (ASM), Correlation, and Variance. These are generated in R Studio using the GLCM package. We set the user-defined parameters of window size (kernel) and shift. Kernels apply a function to the central pixel based on the neighbouring pixels. They, therefore, not only deal with noise in data but also influence the performance of models. Thus, selecting the ones that best fits the data characteristics is essential. Using a scaling factor of two, we use varying kernel sizes ranging from 5X5 to 27X27 for each of the four bands and apply a shift factor of 1. As a result, we have 416 textural bands collectively described as high dimensional data (or big data). To reduce our data's dimensionality and identify the best kernel size for classification, we use the Variable Selection Using RF (VSURF) algorithm, implemented in R Studio (Genuer, Poggi, & Tuleau-Malot, 2015).

For the second land cover/use classification, the hazard index is added as an image feature. For both classifications, Random Forest (RF) is used. Parameter optimization (ntree and mtry) are determined using iterative tuning operations. The first parameter that we tune is ntree, which indicates the number of trees used to build the model. For both land cover and land use classification, the optimal value is determined by starting the value at 0-5000 and varying the intervals by 500 until the learning curves of each predictor class (including OOB samples) stabilizes. While optimizing ntrees, the mtry values are kept at default, i.e., mtry=√number of variables. Mtry represents the number of nodes to be split in each tree. After finding stable values for ntrees, mtry is optimized by varying the value starting with the number of predictor variables.

To perform land cover classification, we identify four classes of land cover in the study area, i.e. built-up, bare land, vegetation and water. Within each category, we further identify sub-classes to capture the diverse nature of our study area. The built-up sub-classes are mentioned in previous sections (high-mid density, low density, deprived type I, deprived type II, including non-residential buildings) (Vanhuysse et al., 2021) (Fig. 6)We use OSM data to automatically generate labelled samples for classes bare land, unpaved roads, and vegetation cover through random sampling. Next, we perform a visual assessment of the samples, and for the class "vegetation" we supplement them with manually labelled samples to encompass the diversity of this class. In total, we generate 1219 labelled samples. These samples are randomly split into 70% for training and 30% for cross-validation and we rely on the out-of-bag (OOB) error to evaluate the model's classification performance.

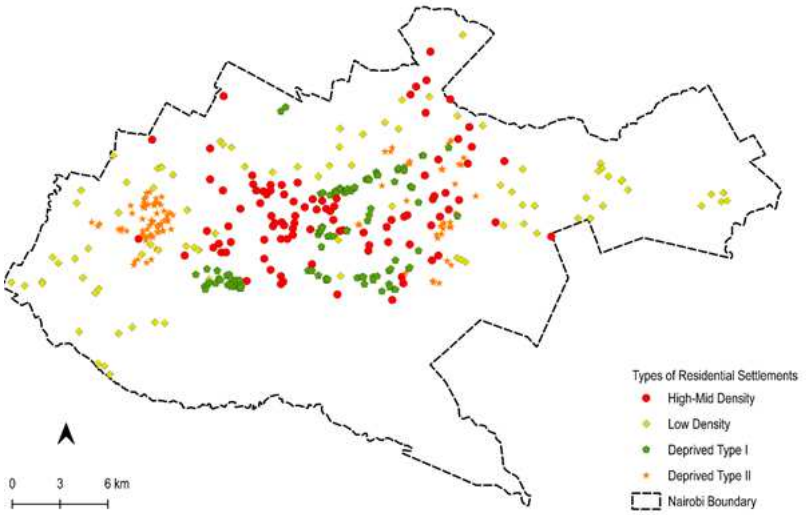

Figure 6: Reference data used for training and validation of the built-up sub-classes.

e. . Quantitative and qualitative validation of results

For the *quantitative validation*, we compute the overall accuracy from the confusion matrix that provides the global accuracy assessment measure based on total correctly classified pixels. Additionally, we compute the F1 score- the weighted average function of precision and recall (Brownlee, 2014). Precision is calculated using the confusion matrix as a ratio of correctly predicted observations to the total predicted positive observations. On the other hand, recall is calculated as the ratio of correctly predicted positive observations to total observations by class.

For the *qualitative* validation of the multi-hazard index, we conduct household surveys in two deprived settlements in Nairobi: Kibera and Kariobangi North. In developing the questionnaire, we focus on the hazards identified in the multi-hazard index. Furthermore, given that the purpose of the questionnaire is to understand the hazards experienced in deprived settlements and at the household level, we use a funnel approach for the survey design (from settlement to household level). The questions are closed-ended with an allowance for additional commentary by the respondents (annex 1). A local community group (Community Mappers) provided research assistant services. A random sampling strategy was employed to reduce bias in the data collection. Specifically, we created grids of 100mx100m over the settlements and using the random selection tool in QGIS, 70 grid cells were selected in Kibera and 30 in Kariobangi North (Fig. 7). The questionnaire was designed and deployed using the KoBo toolbox, which was selected due to its compatibility with mobile devices, geo-location collection capabilities, and is a free and open-source application.

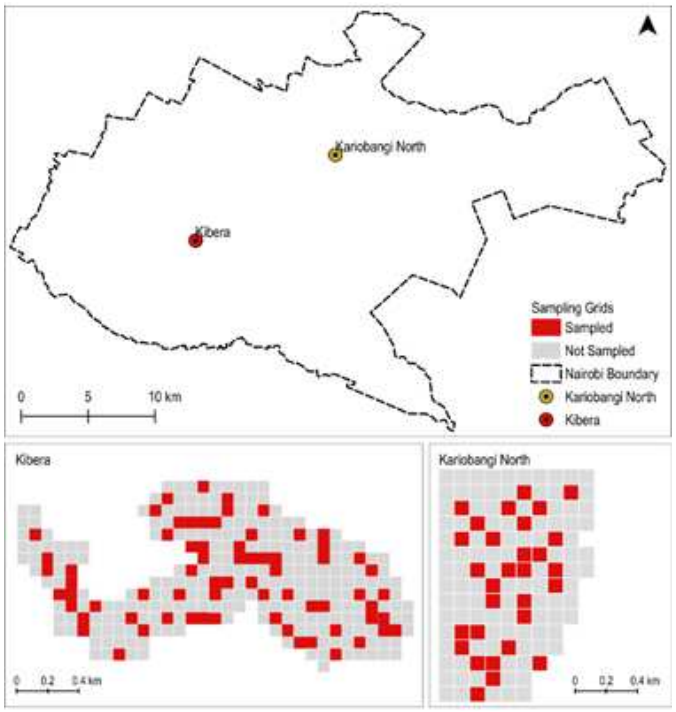

Figure 7: Study area with location of selected settlements for HH survey (top) and randomly selected grids within Kibera (bottom left) and Kariobangi North (bottom right).

3. Results

First, we provide the results of the multi-hazard index per the 10 sub-hazards. Second, two validation approaches of the index are shown, i.e., a quantitative validation by using the hazard index for classifying the location of deprivation areas and a qualitative validation by a household survey in deprived communities.

a. Multi-Hazard Susceptibility Index

We first present the weight distribution of the index, from main hazard category to indicators (Table 3). These were used to compute the multi-hazard index of our study as presented in the following section. While typical multi-hazard assessments rely on occurrence or magnitude data for hazard analysis, the unavailability of these data resulted in the construction of a multi-hazard susceptibility index.

Table 3: Distribution of weights from the hazard categories to indicators as used to compute the multi-hazard index.

Hazard	Weight	Sub-Hazard	Weight	Code	Indicators	Weight
Flood	0.167	Riverine floods	0.0835	F1	Height Above Nearest Drainage (H.A.N.D)	0.042
				F2	Proximity to Rivers	0.042
		Run-off	0.0835	F3	Geomorphons	0.0835
Epidemic	0.167	Epidemic	0.167	E4	Proximity to Garbage dump sites	0.167
Weather and climate	0.167	Extreme temperatures	0.167	W5	Day Land Surface Temperature (LST)	0.0835
				W6	Night Land Surface Temperature (LST)	0.0835
Transport accidents	0.167	Rail accidents	0.0557	T7	Proximity to Railway lines	0.0557
		Road accidents	0.0557	T8	Proximity to major roads	0.0557

		Aero accidents	0.0557	T9	Proximity to Airports	0.0557
Industrial accidents	0.167	Industrial accidents	0.167	J10	Proximity to Industries	0.0835
				J11	Density of industries	0.0835
Biophysical hazards	0.167	Fire	0.0835	B12	Density of buildings	0.0278
				B13	Road density	0.0278
				B14	NDVI	0.0278
		Air pollution	0.0835	B15	Sulphur Dioxide (SO_2)	0.021
				B16	Nitrogen Dioxide (NO_2)	0.021
				B17	Ozone (O_3)	0.021
				B18	Carbon Monoxide (CO)	0.021

Next, we find that Nairobi is highly susceptible to riverine and runoff flooding (Fig. 8). Two factors explain the observed high susceptibility to river inundation of the city. First, parts of the city have a relatively flat terrain. Secondly, the city has three major tributaries (Nairobi, Mathare and Ngong rivers) of the Nairobi Drainage basin system cutting through the city. Despite the seemingly high susceptibility to riverine flooding, the experts inform us that the river tributaries do not pose a significant threat to the city, in general, since the tributaries do not have a big extend and are in valley terrains. However, this is different for deprived settlements since many encroach on the riparian reserves (Fig. 4) and hardly have any protective measures to prevent flooding. On the other hand, runoff flooding appears to be a city-wide threat, including in deprived settlements, as our experts emphasize. Looking at the index, most of the city has scores > 0.6. Specifically, the central and eastern regions of the city are at high risk of runoff flooding. The terrains of these regions are characterized by foot slopes that transition into flat terrain. Furthermore, they lie downstream of the Nairobi drainage system, where the typical slums are mainly located.

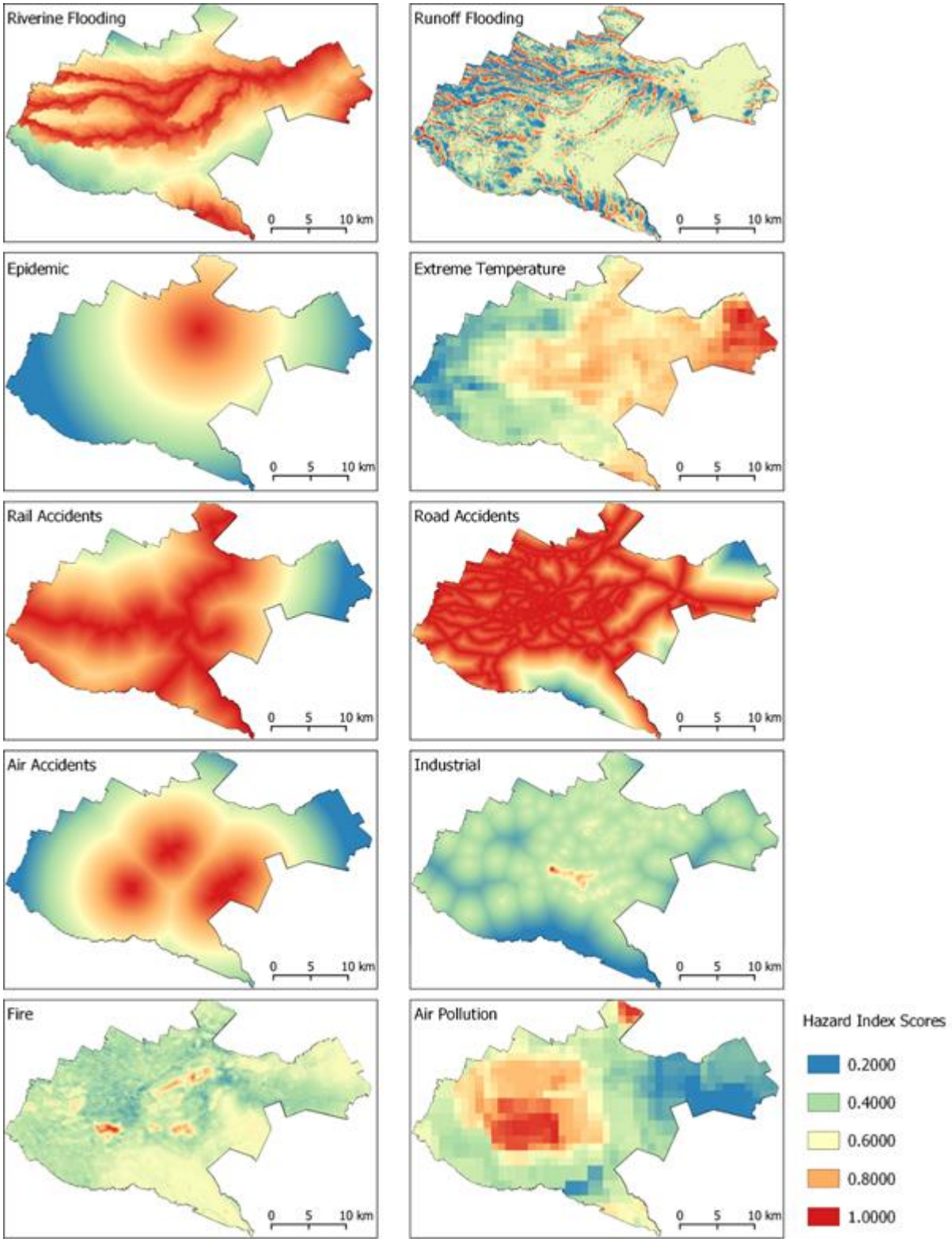

Figure 8: Spatial distribution of hazards in Nairobi per sub-hazard category of the multi-hazard index.

In terms of epidemics, the index is based on the proximity of settlements to the city's sole landfill, located in the north-eastern region. As a result, the hazard susceptibility is higher near the landfill. Extreme temperatures also have a distinct pattern, increasing from west to east (Fig. 8). Climatic factors can explain the sharp contrast between the west and east parts of the city. The western regions are closer to the highland areas (Kiambu County), while the eastern and southern regions are towards the semi-arid climatic zones (Machakos and Kajiado counties). As a result of using proximity measures to transport infrastructures, most of the city has hazard scores >0.8 (Fig.

8). Due to the high connectivity of the road and rail infrastructure, most of the city except the far eastern region is hazardous (Fig. 8). Furthermore, Nairobi is served by three airports located in the city's central areas. The index reflects this pattern, and the urban core and southern regions are thus most susceptible to air transport-related accidents.

Also, industries are spread throughout the city; as a result, the index captures this pattern (Fig. 8). Therefore, we find the risk of industrial hazards is not as high compared to the other assessed hazards. Most of the city has hazards scores of 0.6 and below. However, within the city's core, there is a hotspot area that coincides with the zoned industrial area of Nairobi. Similarly, the fire hazard index highlights distinct hotspots in the city (Fig. 8). Interestingly, the hotspot patterns distinctively outline some commonly known deprived settlements such as Kibera, classified as class 3 - typical slum settlements in this study (see Fig. 7). The distinct pattern for the fire hazard index can be attributed to the district characteristics of deprived settlements, i.e. densely built, lacking adequate road infrastructure and green spaces (all features used to describe the susceptibility to fire hazards). The index further reveals that the central-western region is the most affected by air pollution, spreading to the western, northern and southern areas (Fig. 8). The possible reason for this is that by looking at the annual wind directions, the most predominant winds blow from the northeast direction and hardly any from the west (Windfinder, 2021).

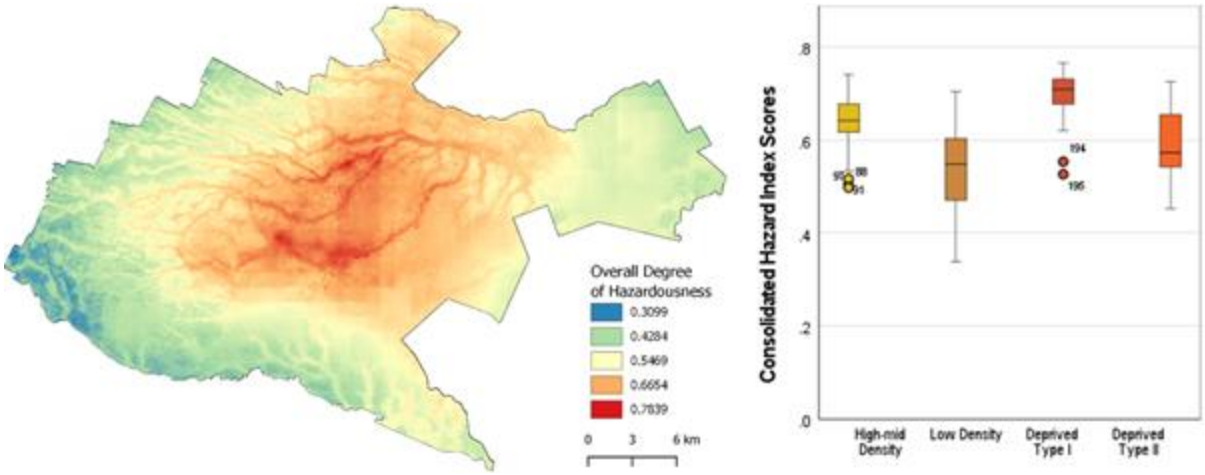

Figure 9: Spatial distribution of hazards in Nairobi. Categories indicate the degree of hazardousness computed from the summation of weighted hazard indicators.

Lastly, to compute the overall hazard index, we summed the weighted indicators. As a result, we find that the urban core of Nairobi is the most hazardous while the western region is the least (Fig. 9). The river tributaries are also highlighted; however, their hazardousness coincides with the overall distribution of hazards in the city. Typical slums are in the most hazardous locations, followed by high-mid density settlements, atypical slums and low-density settlements, respectively.

b. Predicting Deprivation via the Multiple Hazard Index

To test the ability of multi-hazards to predict the location of deprivation, we compared an image-based classification approach that includes textural features (texture-based data set) to a classification approach that uses multi-hazards (multi-hazard dataset). Using the VSURF algorithm to select the best features for predicting deprivation, 35 features of 420 are obtained from the texture-based dataset and seven features of 22 from the multi-hazard dataset. Both datasets obtain overall accuracy of above 70% at 95% confidence. The multi-hazard dataset, however, performs slightly better by 2% OA. These results are obtained with RFC parameters optimized at *ntree*= 2500 and *mtry*=6 for the texture dataset and; *ntree*=3000 and *mtry*=2 for the multi-hazard dataset.

Table 4: A comparison of precision, recall and F1 score per class for multi-hazard and texture-based datasets.

	Multi-Hazard + LCC			Textures + LCC		
	Precision	Recall	F1	Precision	Recall	F1
High-Mid Density	0.73	0.64	0.68	0.74	0.66	0.71
Low Density	0.50	0.58	0.53	0.53	0.83	0.65
Non-Residential	0.99	0.89	0.94	0.63	0.73	0.68
Deprivation Type I	0.85	0.83	0.84	0.84	0.73	0.78
Deprivation Type II	0.68	0.87	0.76	0.59	0.69	0.63
Non-Built	0.71	0.63	0.67	0.93	0.67	0.68

From the multi-hazard dataset, the recall values of the deprived type I and II settlements are the highest (0.84 and 0.87, respectively), following those of non-residential areas (Table 4). The precision value of typical slums is also high (0.85), resulting in a high F1 score of 84%. Despite obtaining low recall values for deprived type II (0.68), the multi-hazard model performs well at classifying deprived settlements, getting an F1 score of 76%. In comparison, the textures model performs slightly poorly at classifying typical slums by obtaining an F1 score of 78% compared to the multi-hazards model. However, when comparing the settlements classes, typical slums are the best classified, followed by high- mid-density settlements (F1 score of 71%) (Table 3).

We further note that the models confuse class prediction of low-density settlements, non-built areas, high-mid density settlements and deprived type II settlements. Based on the multi-hazard model, the low recall values (0.58) of low-density settlements followed by non-built (0.63) and high-mid density (0.64) reflect this (Table 4). We find this to occur because low-density settlements and non-built areas are located in the city's periphery. Also, the data we use has a resolution of 10m; thus, some houses in low-density neighborhoods may go undetected. Additionally, the nature of high-mid density settlements varies within Nairobi, with some regions having similar characteristics to those of low-density settlements (Fig. 5). Looking at the textures dataset, the high-mid density settlements have the lowest recall (0.66), followed by the non-built class (0.67) and deprived type II (0.69). Typically, deprived type II settlements occur both at the city center and the periphery (Fig. 5). As a result, they could be confused with both high-mid density settlements and non-built areas.

Both models perform well at classifying typical slums. The main difference observed is that the multi-hazard dataset better classifies deprived areas than the textures dataset. Also, despite having a high OA, we see from the visual interpretation of the classification that the multi-hazards dataset generalizes entire regions while the textures-based model is noisier (Fig. 10). Thus, the use of hazard-based data highlights the location of deprived areas but provides a generalized map due to the coarse resolution of several inputs.

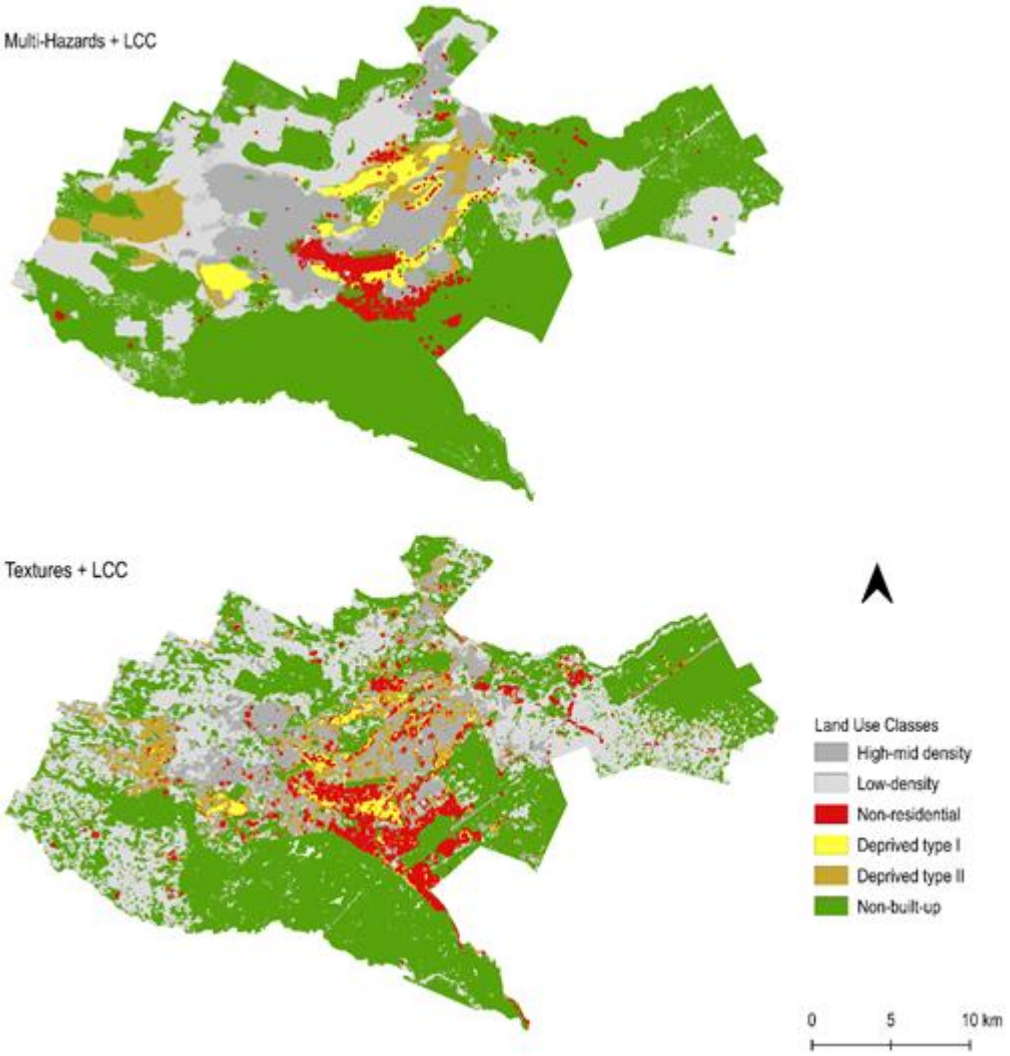

Figure 10: Land use maps (top) generated from the multi-hazard dataset and texture features (bottom).

c. Qualitative Evaluation of Multiple Hazards in Settlements

Our survey was divided into two sections. The first targeted responses of the hazards affecting the respective settlement, and the second focused on the household's individual experiences. The questionnaire captured all identified hazards as per the index, except for air transport-related hazards. Also, there was no differentiation between riverine and runoff flooding (often occurring combined). Furthermore, some of the hazards were disaggregated, according to their plausible causes, e.g., extreme temperatures split to capture the extremities (heat and cold). Lastly, we also included building collapse as a hazard captured by the durable housing domain.

3.3.1. Settlement level

The highest reported hazard in both settlements was garbage accumulation, at 26% in Kariobangi North and 19% in Kibera at the settlement level (Fig. 11&12). For many years, Nairobi has relied on the Dandora landfill, which was declared full 25years ago (UNEP, 2018). Thus, these findings can be attributed to the city's lack of adequate garbage disposal services leading to garbage accumulation within settlements.

Figure 11: Garbage accumulation in the Nairobi River in Kibera, 2019.

In Kariobangi North, disease outbreaks (22%) is the second most reported hazard, followed by air pollution (12%) and fire (11%) (Fig. 12). The three leading causes of disease outbreaks are attributed to inadequate water drainage systems (23%), poor environmental conditions (20%) and burst sewerage pipes (20%). Further, air pollution in Kariobangi North is reportedly caused by burning garbage (44%) and industries (35%), while fire is mainly caused by poor electricity connections (53%) and industrial accidents (24%).

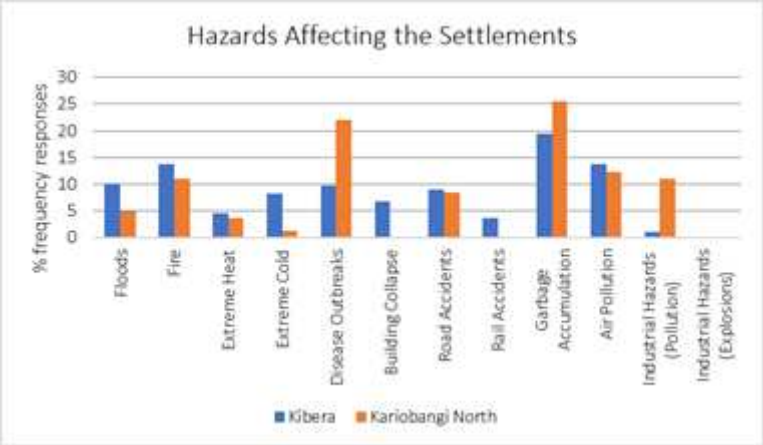

Figure 12: Reported hazards at the settlement level.

In Kibera, air pollution (14%) and fire (14%) are the second-highest reported hazards, followed by floods (10%) and disease outbreaks (10%) (Fig. 12). Like Kariobangi North, burning garbage is the highest cause of air pollution, and poor power connections (60%) is the leading cause of fires in Kibera. The reported causes of flooding are blocked drainage channels (33%), insufficient drainage channels (33%), and proximity to river channels (31%). Disease outbreaks, on the other hand, are linked to several factors, including the reliance on unprotected toilets (19%), bursting of sewerage pipes (18%), poor water drainage systems and poor sanitation and hygiene by households (17%).

3.3.2. Household level

At the household level, garbage accumulation was also the highest reported hazard in both Kibera (32%) and Kariobangi North (35%) (Fig. 13). In Kariobangi North, this is followed by disease outbreaks (26%), fire (12%) and industrial pollution (12%), following a similar trend to reported hazards at the settlement level. In Kibera, extreme cold (21%) is the second-highest hazard, followed by fire (11%) and extreme heat (10%) (Fig. 13). Building collapse is reported only in Kibera and at a low percentage (7%).

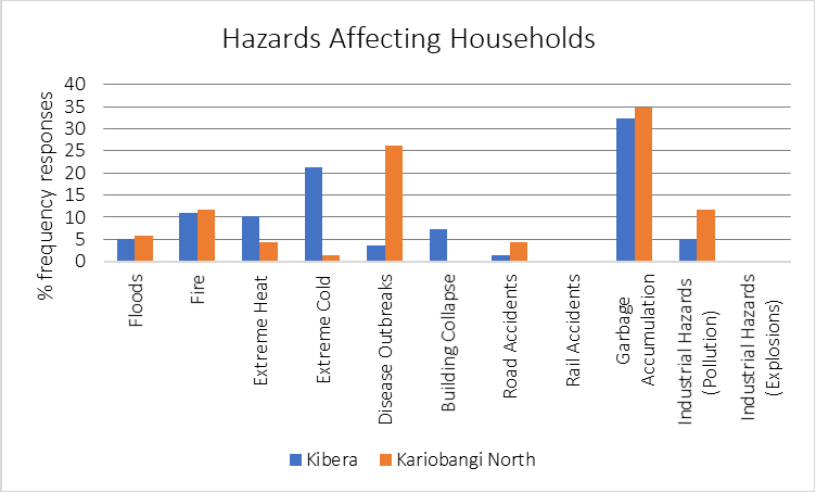

Figure 13: Reported hazards at the household level.

Furthermore, since the durable domain of housing highlights that the quality of structure influences a household's protection against climatic effects, including extreme temperatures, we investigated the relationship between extreme temperatures and the quality of building materials. We found that the common building materials in deprived settlements, as ranked by experts from most to least durable, are: quarry stone, brick, mud-with concrete plastering, mud, corrugated iron sheets, tin, polythene and cardboard. Also, the rent of dwellings differs based on the type of materials used. The more durable the building materials, the higher the cost of housing rent (Fig. 14).

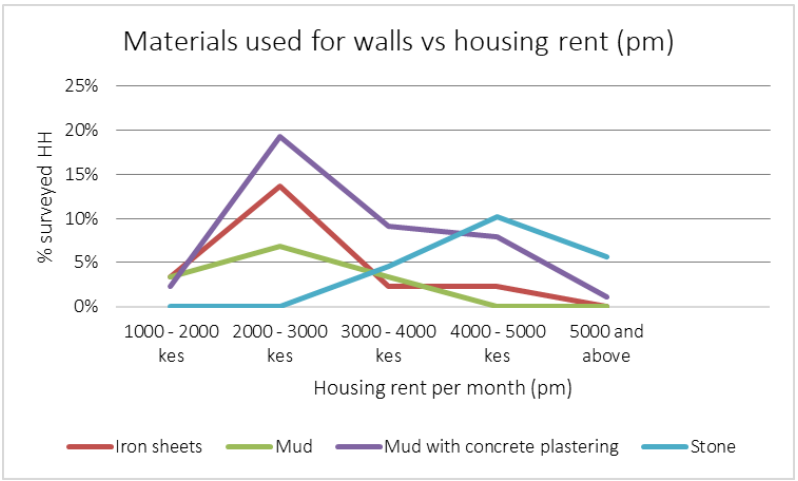

Figure 14: Comparison between building material and rent.

To understand the interaction between the hazards and building quality at the household level, we asked the respondents the reason as to why they were affected by reported hazards based on four household dwelling characteristics: roofing, walls, floor, and geographic location. For the hazards reported at the household level but not at the settlement level (extreme heat, extreme cold and building collapse), we found the type of flooring (34%) as the highest cause of extreme cold, closely followed by the type of walls (30%). Upon investigating the type of

floor and wall material of by reporting household, we find that 53% have concrete plastering as they type of floor material and 53% have iron sheets for walls. Also, all households reporting extreme heat had iron sheets for walls. On the other hand, the majority (50%) of households reporting building collapse had mud walls (without modifications) followed by mud walls with concrete plastering 38%.

We, therefore, found that no household with the more durable housing materials (quarry stone, bricks, mud) was affected by extreme temperatures. On the other hand, those affected by extreme temperatures mainly had corrugated iron sheets for either roofing or walls that typically have poor insulating properties. Further, referencing the monthly rent, we see that the poorer households are most affected by extreme temperatures. These findings further support claims made in the literature that the quality of the housing structures in deprived areas is often precarious and offers insufficient protection from climate and weather elements (UN-Habitat, 2015).

3.3.3. Comparison of Multi-hazard Index scores between 2 settlements

We further explored the degree of hazardousness of the two deprived settlements' surveyed in this study, as captured by the multi-hazard index (Fig. 15). The highest hazards threats are transport accidents and riverine flooding, similar to the city level. However, both settlements have hazard scores of 0.8, higher than the city's average (Fig. 15). On the contrary, the qualitative analysis did not highly report these hazards. Only 9% of the respondents reported road accidents in both settlements at the settlement level. Additionally, rail accidents (4%) were only reported in Kibera. At the household level, there was only 2% and 4% reporting on road accidents in Kibera and Kariobangi North, respectively; and none for rail accidents. These findings highlight the limitations of the index to localize the hazards. Furthermore, in contrast to our initial findings, the atypical slum - Kariobangi North had a higher overall degree of hazardousness than the typical slum – Kibera (Fig.15).

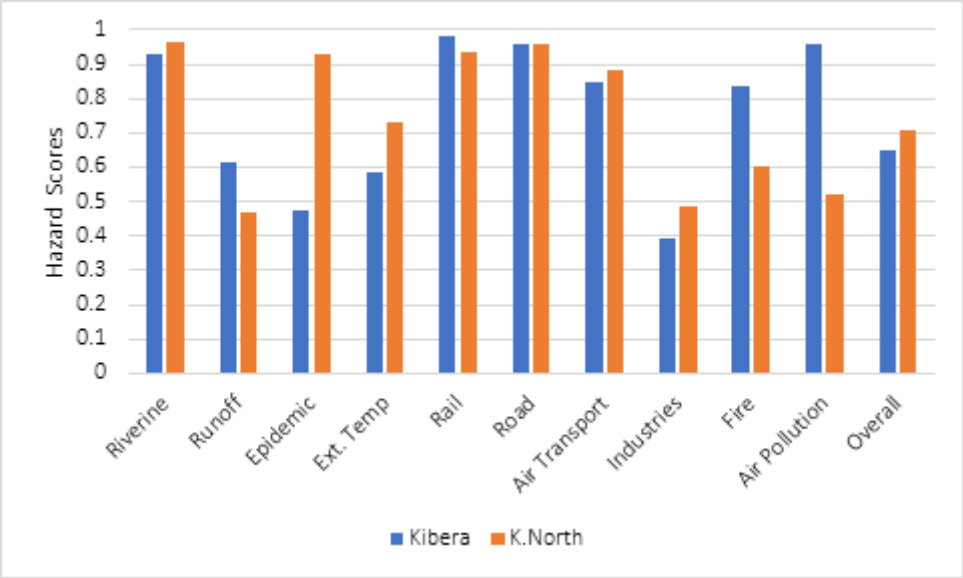

Figure 15: Comparison of settlements multi-hazard index scores.

Nevertheless, we note that (in exemption of the hazards that are high at the city-level), the other highly scoring hazards in the two settlements were also highly reported at the settlement and household levels. Of the hazards identified by the index with scores >0.8 in Kariobangi North, the epidemics have higher values than Kibera and are above the city's average (Fig. 15). When contrasting these findings to the settlement and household level assessments, we find that in Kariobangi North, garbage accumulation is the most reported hazard at settlement and household levels, followed by disease outbreaks (Fig. 12&13). Both hazards are indicative of susceptibility to epidemics. Furthermore, while the index outcome is due to the settlement's proximity to the city's landfill, the challenges are more localized at the settlement level; the causes are linked to the high accumulation of garbage and infrastructure failures. In Kibera, air pollution and fire are the identified hazards with index scores

significantly higher than the city's average and Kariobangi North (Fig. 12). Similarly, at the settlement and household levels, we found that following garbage accumulation, air pollution, and fire was the highest reported hazards at the settlement level and extreme cold, followed by fire at the household level (Fig. 12&13).

4. Discussion

The settlements' spatial distribution suggest that typical slums are the most vulnerable to the identified hazards in this study. Below we discuss the outcomes of the multi-hazard index and qualitative analysis by contrasting the settlement classes per sub-hazard category.

a. Validation of Multi-Hazard Index

In assessing the settlements exposure o multi-hazards, we found typical slums to be the most exposed settlements in all sub-hazard categories used in this study (Fig.16). Specifically, we see that typical slums are most susceptible to fire hazards and runoff flooding compared to the other settlements. Looking at fire hazards, we further find atypical slums as the second most exposed settlements. These findings agree with expert opinions and literature that state that urban fires are frequent in deprived settlements within Nairobi. The fire outbreaks are attributed to several factors, including poor power connections and drunkenness (Ngau & Boit, 2020). In addition to the causes, slum conditions intensify fire outbreak incidents due to their high density and compactness; lack of open spaces to provide safety; and combustible building materials (Ngau & Boit, 2020). The poor road connectivity further hinders responses to the fires within the settlements (Ngau & Boit, 2020).

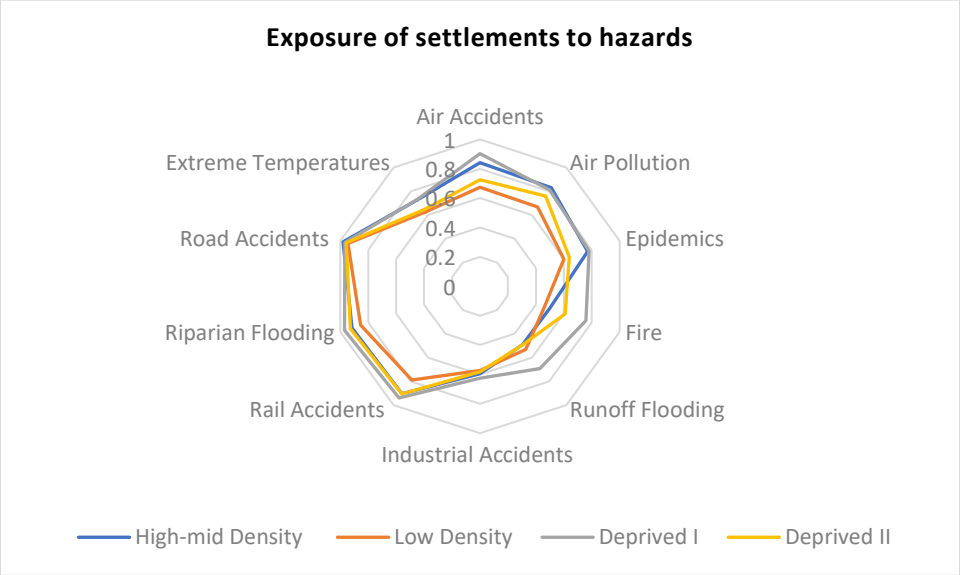

Figure 16: Settlements exposure to hazards.

On the other hand, the experts consider runoff flooding a city-wide problem. On the contrary, our study finds that in comparison to other hazards, runoff flooding is not a significant threat to the city. We find this to be due to the data used for assessing the hazard. While our study's assessment of runoff flooding was based solely on the physical factors (terrain), other factors causing runoff flooding in the city, i.e., blockage of drainage systems by garbage and lack of adequate drainage systems, were identified by the experts and re-iterated by the survey outcomes. Specifically, blocked drainage channels were reported as the leading cause of flooding in both settlements (57% in Kariobangi North and 33% in Kibera). Insufficient drainage channels (33%) was also reported

in Kibera. Interestingly, we found that Kariobangi North is also affected by point source runoff due to its proximity to the city's sewerage treatment plant inlets (14%).

Second, to typical slums, high-mid density settlements were highly exposed to hazards (Fig.16). Specifically, air transport accidents, extreme temperatures, air pollution, and epidemics hazard threats are predominant. Generally, these settlements – similar to typical slums - are located in the city's central region (Fig. 6). In contrast, low-density settlements have the lowest exposure to hazards followed by atypical slums since they are predominantly located in the city's periphery. Due to more intensive land use and land cover changes, urban cores often experience micro-climate modifications known as Urban Heat Island (UHI), where the temperatures are higher than their surroundings (Seto & Shepherd, 2009; Zhou, Zhao, Zhang, Sun, & Liu, 2015). Air pollution values also tend to be higher due to more industrial activities and less vegetation cover, and lastly, it is where the city's major infrastructures, e.g. airports, are found. In addition to this, the study reveals the interrelations among some of these hazards. For instance, the leading causes of air pollution in Kibera were: the burning of garbage (74%) and pollution emanating from transport activities (14%). The respondents also associated industrial accidents with pollution (air, water, land/soil contamination, noise). In Kariobangi North, industries were reported at 35% as the cause of air pollution in the settlement. These interrelations emphasize the need for an integrated approach to investigating and managing hazards.

Generally, the multi-hazard index found that the most significant threats in Nairobi are road accidents, riparian flooding and rail accidents, respectively (Fig.16). The proximity to transport modes poses a high risk of accidents that may cause injuries and fatalities. In Kenya, reported causes of road accident fatalities in a recent study are attributed to driver-related causes such as 'running over victims' (Muguro, Sasaki, Matsushita, & Njeri, 2020). From this, we infer that secondary causes influence the occurrence of road accidents that our index did not capture. Even though only 9% of the respondents in each settlement reported road accidents, we find that insufficient/lack of pedestrian crossings is the major cause (44% - Kibera and 43% - Kariobangi North). Proximity to transport lines (43%) was the second most reported cause reported in Kariobangi North (43%) and Kibera (42%). The third-highest reported cause of transport accidents is poorly trained/untrained motorcycle riders (14%) in Kariobangi North and inadequate road networks (14%) in Kibera. Similar reasons were reported for rail accidents.

Further, in agreement with the literature (see UN-Habitat, 2015), our study found that deprived areas are affected by hazards due to two main reasons: their location and the quality of the structure. Both are factors tied to the residents' socio-economic status and highlight a crucial trade-off between hazard exposure and access to opportunities such as wealth, industries, markets, and mobility systems for the urban poor. In both Kibera and Kariobangi North, the main reasons for living in the settlement were the closeness to opportunities and rent affordability (Fig. 17). The household survey shows that the housing rent per month in both settlements are significantly low compared to the reported median urban rental expenditures of approx.300USD in Kenya (KNBS, 2018). The cost of monthly rent was lower in the typical slum – Kibera (approx. 20-30 USD) than in the atypical slum – Kariobangi North (approx. 40-50 USD). Therefore, typical slums are most afflicted, and this is highlighted not just by their exposure to hazards but also their socio-economic status.

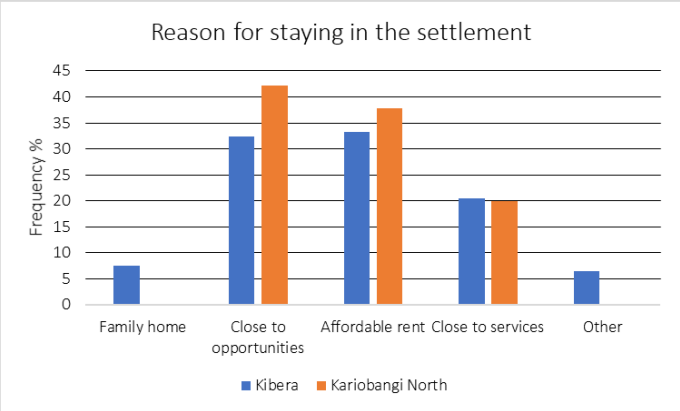

Figure 17:Reasons for staying in a deprived settlement.

In conclusion, despite the difference in reporting of hazards at the three spatial scales (city, settlement and household levels), our assessments captured many similarities. Notably, we found that the city-wide multi-hazard index is a useful starting point for more localized hazard assessments. Additionally, our study demonstrated that geospatial data, specifically EO data and its derivatives produced at high spatial scales and capturing different environmental phenomena, can be utilized in data-poor cities. Further, despite the top-down nature of geospatial methods, our study demonstrates that bottom-up approaches, e.g. household surveys, are still required. Physical and social scientific approaches are complementary and create a necessary feedback loop to improve and refine traditional top-down scientific methods.

b. Predictability of Deprivation Using Multi-Hazards

Interestingly, the multi-hazards model was better at discriminating deprived settlements, whereas the textural feature-based model performed well across settlement discrimination. Specifically, our study demonstrates that open geospatial data is useful in assessing urban poverty, as our attempts at using multi-hazard datasets to map deprivation resulted in high model accuracies. Further, the experiment revealed the layered nature of deprivation that goes beyond the socio-economic conditions of the urban poor but also stresses the hazardous environmental conditions that they live in.

5. Conclusion

The main goal of our study was to test the assumption that deprived areas are dominantly the locations with higher susceptibility to multiple hazards. We find this true from the multi-hazard index and the prediction of deprivation via multi-hazards. Furthermore, by distinguishing the settlements into classes, we establish that typical slums are the worst afflicted by hazards, highlighting the intra-city socio-spatial marginalization. Additionally, rampant marginalization is unveiled by investigating the hazards at the settlement and household levels. We also discovered that intra-settlement marginalization is pegged on the socio-economic status of the residents. In concatenating these findings, we conclude that the poorest urban populations dominantly live in the most hazardous locations.

Although we obtained meaningful results, the present study is not without limitations, to be addressed in future research. First, it was challenging to identify spatial data indicative of hazards, including coherent frequency, magnitude, or occurrence. As a result, we used hazard proxies to create a multi-hazard susceptibility index that mainly highlights exposure to hazards. Nonetheless, a susceptibility index has proven to be a helpful starting point for localized hazard assessments, especially in LMIC's where data availability may be challenging. It is also simple to implement and replicate in other cities. Secondly, as shown by the household responses, we acknowledge that more and better proxies can be identified for the hazards. Lastly, the interrelated nature of some of the hazards highlights the need for more interdisciplinary and integrated approaches to investigating and managing hazards.

6. References

Dilley, M., Chen, R. S., Deichmann, U., Lerner-Lam, A. L., Margaret, A., Jonathan, A., … Yetman, G. (2005). Natural Disaster Hotspots: A Global Risk Analysis. In *World bank*. https://doi.org/10.1002/j.1834-4461.1948.tb00495.x

EM-DAT. (2009). General Classification . Retrieved June 16, 2020, from EM-DAT: The International Disaster Database website: https://www.emdat.be/classification

Greiving, S. (2006). Integrated Risk Assessment of Multi-Harards: A New Methodology. In *Geological Survey of Finland, Special Paper* (Vol. 42).

KNBS. (2018). *Basic Report on Well-being in Kenya -Based on the Kenya Integrated Household Budget Survey (KIHBS)*. Nairobi.

Kohli, D., Sliuzas, R., Kerle, N., & Stein, A. (2012). An ontology of slums for image-based classification. *Computers, Environment and Urban Systems*, *36*(2), 154–163. https://doi.org/10.1016/j.compenvurbsys.2011.11.001

Kuffer, M., Thomson, D. R., Boo, G., Mahabir, R., Grippa, T., Vanhuysse, S., … Kabaria, C. (2020). The role of earth observation in an integrated deprived area mapping "system" for low-to-middle income countries. *Remote Sensing*, *12*(6). https://doi.org/10.3390/rs12060982

Kuffer, M., Wang, J., Nagenborg, M., Pfeffer, K., Kohli, D., Sliuzas, R., & Persello, C. (2018). The Scope of Earth-Observation to Improve the Consistency of the SDG Slum Indicator. *ISPRS International Journal of Geo-Information*, *7*(11), 428. https://doi.org/10.3390/ijgi7110428

Muguro, J. K., Sasaki, M., Matsushita, K., & Njeri, W. (2020). Trend analysis and fatality causes in Kenyan roads: A review of road traffic accident data between 2015 and 2020. *Cogent Engineering*, *7*(1), 1797981. https://doi.org/10.1080/23311916.2020.1797981

Ngau, P. M., & Boit, S. J. (2020). Community fire response in Nairobi's informal settlements. *Environment and Urbanization*, *32*(2), 615–630. https://doi.org/10.1177/0956247820924939

Pamoja Trust. (2009). *An Inventory of the Slums in Nairobi*. Retrieved from http://www.irinnews.org/pdf/nairobi_inventory.pdf

Ramin, B. (2009, December). Slums, climate change and human health in sub-Saharan Africa. *Bulletin of the World Health Organization*, *87*(12). https://doi.org/10.2471/BLT.09.073445

Revi, A., David E., S., Aragón-Durand, F., Corfee-Morlot, J., Kiunsi, R. B. R., Pelling, M., … Solecki, W. (2014). Urban areas. In C. B., V. R. Barros, D. J. Dokken, K. J. Mach, M. D. Mastrandrea, T. E. Bilir, … L. L. White (Eds.), *Climate Change 2014: Impacts, Adaptation, and Vulnerability. Part A: Global and Sectoral Aspects. Contribution of Working Group II to the Fifth Assessment Report of the Intergovernmental Panel on Climate Change* (pp. 535–612). Cambridge, United Kingdom and New York, NY, USA: Cambridge University Press.

Seto, K. C., & Shepherd, J. M. (2009). Global urban land-use trends and climate impacts. *Current Opinion in Environmental Sustainability*, *1*(1), 89–95. https://doi.org/10.1016/j.cosust.2009.07.012

Thomson, D. R., Kuffer, M., Boo, G., Hati, B., Grippa, T., Elsey, H., … Kabaria, C. (2020). Need for an integrated deprived area "slum" mapping system (IDEAMAPS) in low-and middle-income countries (LMICS). *Social Sciences*, *9*(5), 1–17. https://doi.org/10.3390/SOCSCI9050080

UN-Habitat. (2015). *Slum Almanac 2015/2016: Tracking Improvent in the Lives of Slum Dwellers*. Retrieved from https://unhabitat.org/slum-almanac-2015-2016

UNEP. (2018, December 21). Smoking Nairobi landfill jeopardizes schoolchildren's future. Retrieved June 15, 2021, from Cities and lifestyles website: https://www.unep.org/news-and-stories/story/smoking-nairobi-landfill-jeopardizes-schoolchildrens-future

Wekesa, B. W., Steyn, G. S., & Otieno, F. A. O. (2011). A review of physical and socio-economic characteristics and intervention approaches of informal settlements. *Habitat International*, *35*(2), 238–245. https://doi.org/10.1016/j.habitatint.2010.09.006

Windfinder. (2021, June). Monthly wind direction and strength distribution. Retrieved August 5, 2021, from Wind & weather statistics Nairobi/Jomo Kenyatta website: https://www.windfinder.com/windstatistics/nairobi-jomo-kenyatta-airport

Zhou, D., Zhao, S., Zhang, L., Sun, G., & Liu, Y. (2015). The footprint of urban heat island effect in China. *Scientific Reports*, *5*(1), 11160. https://doi.org/10.1038/srep11160